Front. Med.
https://doi.org/10.1007/s11684-019-0726-4

REVIEW

Survey on deep learning for pulmonary medical imaging

Jiechao Ma[1,*], Yang Song[2,*], Xi Tian[1], Yiting Hua[1], Rongguo Zhang[1], Jianlin Wu (✉)[3]

[1]*InferVision, Beijing 100020, China;* [2]*Dalian Municipal Central Hospital Affiliated to Dalian Medical University, Dalian 116033, China;* [3]*Affiliated Zhongshan Hospital of Dalian University, Dalian 116001, China*

Abstract **As a promising method in artificial intelligence, deep learning has been proven successful in several domains ranging from acoustics and images to natural language processing. With medical imaging becoming an important part of disease screening and diagnosis, deep learning-based approaches have emerged as powerful techniques in medical image areas. In this process, feature representations are learned directly and automatically from data, leading to remarkable breakthroughs in the medical field. Deep learning has been widely applied in medical imaging for improved image analysis. This paper reviews the major deep learning techniques in this time of rapid evolution and summarizes some of its key contributions and state-of-the-art outcomes. The topics include classification, detection, and segmentation tasks on medical image analysis with respect to pulmonary medical images, datasets, and benchmarks. A comprehensive overview of these methods implemented on various lung diseases consisting of pulmonary nodule diseases, pulmonary embolism, pneumonia, and interstitial lung disease is also provided. Lastly, the application of deep learning techniques to the medical image and an analysis of their future challenges and potential directions are discussed.**

Keywords deep learning; neural networks; pulmonary medical image; survey

Introduction

Deep learning covers a set of artificial intelligence methods that use many interconnected units to fulfill complex tasks. Deep learning algorithms can automatically learn representations from large amounts of data rather than the use of a set of pre-programmed instructions [1–3]. Radiology is a natural application field for deep learning because it relies mainly on extracting useful information from images, and the research in this field has rapidly developed [4]. With the aggravation of air pollution and the increasing number of smokers, respiratory diseases have become a serious threat to people's life and health [5]. However, many of the early clinical manifestations of respiratory diseases are not evident, and some patients do not even feel any discomfort during the early stage. Hence, many patients miss the critical period of early treatment because they discover clinical symptoms at a later time. Therefore, public awareness of early detection and treatment is necessary for the prevention and treatment of lung diseases. In medical imaging, the accurate diagnosis and evaluation of diseases depend on image collection and interpretation. Computer-aided diagnosis (CAD) of medical images has been developed for the early discovery and analysis of patient's symptoms based on medical images. However, this method has long been rooted on limited features that are identified based on physicians' past experiences. Most researchers also study medical image features that need to be extracted manually and thus require special clinical experience and a deep understanding of the data [6,7]. With the rapid development of computer vision and medical imaging, computer-aided calculation can assist medical workers in diagnosis, such as enhancing diagnostic capabilities, identifying the necessary treatments, supporting their workflow, and reducing the workload to capture specific features from medical images.

The deep learning algorithm was first applied to medical image processing in 1993, in which the neural network was used for the detection of pulmonary nodules [8]. In 1995, deep learning was applied in breast tissue detection [9]. The region of interest (ROI) was extracted from mammograms through a model, which contains tumors and normal tissues confirmed via biopsy. The model results include one input layer, two hidden layers, and one output layer for back propagation. At that time, the typical convolutional

Received July 18, 2019; accepted October 12, 2019

Correspondence: Jianlin Wu, cjr.wujianlin@vip.163.com

*These authors contributed equally to this work.

neural network (CNN) image-processing architecture has not been widely accepted by scholars because it has high demand for computing power and sufficient data and does not provide good interpretations of results. Most doctors prefer clear interpretations, which are important in the medical field but cannot be provided by deep learning to support clinical decisions.

Most people focus on manual feature extraction on images, such as features that may represent the edge of a straight line (e.g., organ detection) or contour information (e.g., a circular object like a colon polyp) [10]. Alternatively, key points (feature points) on different scales are identified, and their directions are calculated [11,12]. Radiomics [13] is also used to study some higher-order features, such as the local and global shape and texture.

With the explosive growth of data and the emergence of graphics processing unit with increasing computing power, deep neural networks have made considerable progress. In general, medical image processing can be divided into image classification, detection, segmentation, registration, and other related tasks. For image classification, each image must be classified into specific categories. The algorithm determines related objects in the image, including the type of disease, pneumothorax, and bullae and generates a list of possible object categories in descending order of confidence [14–17]. The image object detection is a further improvement based on image classification. In this task, the algorithm gives the category of the detected object (e.g., pulmonary nodules appear in a CT slice) and marks the corresponding boundary of the object on the image [18–20]. Semantic segmentation is a basic task in computer vision in which visual input is divided into different semantically interpretable categories. All the pixels belonging to the lesion in the image might need to be distinguished [21,22].

Medical image processing mainly aims to detect possible lesions and tumors because of their remarkably effects on the follow-up diagnosis and treatment. Although tumor detection and analysis have been widely studied, many obstacles must be overcome for future application. In pulmonary nodules [23,24], challenges exist due to within-class variability in lesion appearance. First, the shape, size, and density of the same lesion may vary, and the appearance of the lesion might be different (Fig. 1A, solid pulmonary nodules; Fig. 1B, ground glass pulmonary nodules, in green box). Second, many different diseases (normal tissues and pulmonary nodules) show the same texture features (Fig. 1C, pleural nodules, in green box, and many blood vessels in the center of the image). Third, the quality of image acquisition, such as the change of posture, blur, and occlusion, is considered (Fig. 1D). Fourth, different surrounding environments make different types of lung nodules appear to be diverse. Lastly, unbalanced data often pose a challenge in designing effective models from limited data.

Several dedicated surveys have been developed for the application of deep learning in medical image analysis [11,25]. These surveys include a large amount of related works and cover various references in almost all fields in medical imaging analysis by using deep learning. In the present study, we focused on a comprehensive review of pulmonary medical image analysis. A previous review [26] centered on the detection and classification of pulmonary nodules by using CNNs. However, additional works should be focused on targeting the segmentation tasks crossing diverse pulmonary diseases. The present review aimed to present the history of deep learning and its recent applications in medical imaging, especially in pulmonary diseases, and to summarize the specific tasks in these applications.

This paper is organized as follows. In section "Overview of deep learning," we present a brief introduction of deep learning techniques and the origins of deep learning in neuroscience. The specific application areas of deep learning are presented in section "Deep learning in pulmonary medical image." Detailed reviews of the datasets and the performance evaluation are presented in section "Datasets and performance." Finally, our discussion are provided in sections "Challenges and future trends" and "Conclusions."

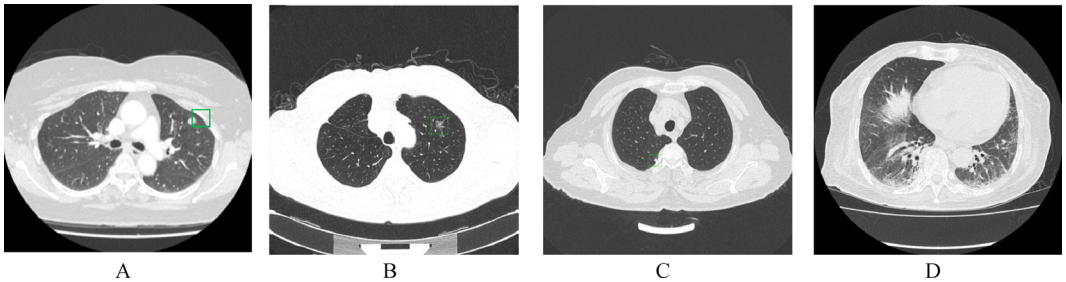

Fig. 1 Variety of lesion appearances poses a big challenge for medical image processing. (A) Solid nodule (green box), (B) ground glass nodule (green box), (C) pleural nodule (green box), and (D) the effect of image acquisition.

Overview of deep learning

In this section, we introduce the origin of modern deep learning algorithms and several deep learning network structures commonly used in medical image processing. Then, we will briefly introduce some concepts used in the network (Table 1).

Historical perspective on networks

The history of neural networks can be traced back to the 1940s, and the deep neural network at that time was called cybernetics [27–29]. Simple bionic models such as perceptrons, which can train a single model, have emerged with the discovery of the biomedical theory [30]. In 1962, Hubel and Wiesel proposed the concept of the receptive field by studying of cat visual cortical cells and found that the animal's visual nervous system recognizes objects in layers [21,32]. A simple structure of visual processing was then established. When an object passes through a visual area, the brain constructs complex visual information through the edges. Although this model helps understand the functions of the brain, it was not designed to be an actual model. In 1971, basing on the receptive field study, Blakemore [33] proposed that receptive field of visual cells is acquired rather than innate.

In 1980, Japanese scholar Fukushima proposed a new cognitive machine (neocognitron) based on the concept of receptive field. It can be regarded as the first implementation network of CNN and the first application of the concept of receptive field in the field of artificial neural network [34]. The model is inspired by the animal visual system, namely, the hierarchical structure of vision proposed by Hubel. In 1984, Fukushima proposed an improved neocognitron machine with double C-layers [35]. By the 1980s, the method of connection mechanism was introduced [36]. Rumelhart proposed the famous back-propagating (BP) algorithm, which can train a neural network with two hidden layers and transmit errors in reverse for changing the weight of the network [37]. Some of the ideas of this algorithm have been applied in the structure of deep networks. The emergence of BP algorithm makes multi-layer perceptrons trainable and solves XOR problems [38] that cannot be explained by a single perceptron [39,40]. In 1989, Robert Hecht–Nielsen reported that a continuous function in any closed interval can be approximated using a three-layer network of hidden layers, indicating that the multilayer perceptron has the so-called "universal approximation" capability [41].

Modern architectures

These simple learning algorithms mentioned in the previous section have greatly accelerated the development of neural networks. In 1989, the emergence of CNNs made people pay attention to the generalization error of networks [43,44,49]. In 1990, the proposed convolutional network to identify numbers marked the great success of CNNs in the field of computer vision and image processing [44,50]. LeNet [44] was proposed by LeCun in 1998 to solve the problem of handwritten numeral recognition. Subsequently, the basic architecture of CNN has been defined;

Table 1 Historical perspective on networks

Authors	Year	Model name	Main method
Hubel *et al*. [31]	1962	–	Proposed the concept of receptive field and found that the animal's visual nervous system recognizes objects in layers
Blakemore [33]	1971	–	Receptive field of visual cells is acquired rather than innate
Fukushima *et al*. [34]	1980	Neocognitron	First implementation network of CNN and first application of the concept of receptive field
Fukushima *et al*. [35]	1984	Neocognitron	Neocognitron machine with double C-layers
Rumelhart *et al*. [42]	1988	–	Proposed the BP algorithm
Hecht-Nielsen *et al*. [41]	1989	–	Demonstrated that a continuous function in any closed interval can be approximated using a three-layer network of hidden layers
LeCun [43]	1989	CNN	Use of weight sharing and SGD in network optimization
LeCun *et al*. [44]	1998	LeNet	Defined the basic architecture of CNN
Hinton *et al.* [45]	2006	DBN	Improved the difficulty of training the network
Krizhevsky *et al*. [46]	2012	AlexNet	Dropped the top five error rate of the highest accuracy from 26.1% to only 15.3%
Simonyan *et al*. [47]	2014	VGG-Net	VGG can be seen as a deepened version of AlexNet (19 layers)
Szegedy *et al*. [16]	2014	GoogLeNet	Deepening the network (22 layers) and introducing Inception structure instead of simple convolution
He *et al*. [17]	2015	ResNet	Residual module, a design of residual network, allows the network to be trained more deeply (152 layers)
Huang *et al*. [48]	2016	DenseNet	Dense connection: alleviating the problem of gradient disappearance and enhancing feature propagation

it comprises a convolution layer, a pooling layer and a full connection layer.

With the rapid development of computer technology, the computational bottleneck in the neural network has been continuously overcome, which promoted the rapid development of neural networks in the last two decades. Subsequently, the neural network continued to achieve impressive performance on certain tasks, but these network frameworks are still difficult to train [51,52]. Until 2006, the deep belief network proposed that the difficulty of training of neural network was gradually improved [45]. In this network, Hinton uses a greedy algorithm for layer-by-layer training, which effectively solves the above problems. After that, the same strategy was used in training many other types of deep networks [53].

Since 1980, the recognition and prediction capabilities of deep neural networks have improved, and their application fields have become more extensive. With the increasing amount of data, the scale of the neural network model has also expanded tremendously. Among these models, AlexNet can be considered as the landmark algorithm structure [46]; this model was proposed by Krizhevsky in ImageNet in 2012 [54]. Prior to AlexNet, only a single object in a very small image could be identified due to computational limitations. After 2012, the size of the image that the neural network can process has gradually increased, and an image of any size may be used as input for processing. In the same year, in the annual image classification competition ImageNet, AlexNet dropped the top five error rate with the highest accuracy from 26.1% to only 15.3%, which was 10% lower than the previous year's champion and far exceeded the second participating team. Subsequently, many scholars have re-examined deep neural networks. Deep neural convolution networks have often won in this competition. The VGG-Net [47] and GoogLeNet [16] were proposed in 2014, and the 2015 champion algorithm ResNet [17] deepened more layers than the previous network of AlexNet. As the network deepens, it becomes a better network. Dense neural networks [48] have also achieved good results in other fields.

Deep learning in medical image analysis

The aforementioned networks are mainly used for common image classification tasks. An overview of network structures used for classification, detection, and segmentation tasks for the perspective of medical image analysis is described below.

Classification

The classification task determines which classes an image belongs to. Depending on the task, the class can exist in binary (e.g., normal and abnormal) or multiple categories (e.g., nodule classification in chest CT). Many medical studies use CNNs to analyze medical images to stage disease severity in different organs [55]. Some authors investigated on combination of local information and global contextual information and designed architecture for image analysis at different scales [56]. Some work focused on the utilization of 3D CNN for enhanced classification performance [57].

Detection

Object detection in medical image analysis refers to the localization of various ROIs such as lung nodules and is often an important pre-processing step for segmentation tasks in medical image analysis. The detection task in most medical image analysis requires the processing of 3D images. To utilize deep learning algorithm for 3D data, Yang *et al*. processed 3D MRI images by using 2D MRI sequences with typical CNN [58]. de Vos *et al*. localized 3D bounding box of organs by analyzing 2D sequences from 3D CT volume [59]. To reduce the complexity of 3D images, Zheng *et al*. decomposed 3D convolution as three 1D convolutions for the detection of carotid artery bifurcation [60].

Segmentation

Segmentation of meaningful parts, such as organ, substructure, and lesion, provides a reliable basis for subsequent medical image analysis (Fig. 2). U-net [61] published by Ronneberger *et al*. has become the most well-known CNN architecture for medical image segmentation from very few images. U-net is based on fully convolutional networks (FCN) [62]. FCN can be utilized for classification at the pixel level and use deconvolution layer for upsampling the feature map of the last convolution layer and restore it to the same size of the input image, thus allowing the prediction to be generated for each pixel. The spatial information in the original input image is preserved. Subsequently, the pixel-by-pixel classification is performed on the upsampled feature map to complete the final image segmentation. In U-net, however, skip connections are used for connecting downsampling to upsampling layers, which makes features extracted by downsampling layers passed directly to the upsampling layers. This process allows U-net to analyze the full context of the image, resulting in segmentation map in an end-to-end way. After U-net was proposed, many researchers have used U-net structure for medical image segmentation and made improvements based on U-net. Cicek *et al*. designed 3D U-net [63] targeting 3D image sequences, and Milletari *et al*. proposed a 3D-variant of U-net architecture, namely V-net [64], which uses Dice coefficient as loss function.

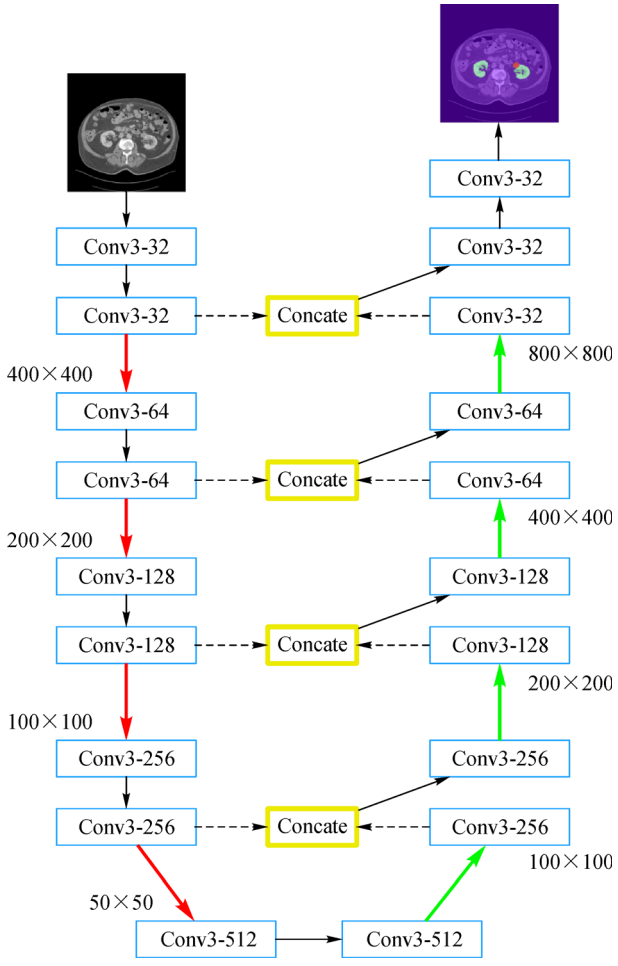

Fig. 2 Structure of segmentation network. The left part uses convolution for the extraction of features, and the right part uses deconvolution for the recovery of the original size. The middle part contains skipping connections that are used in U-net.

Deep learning in pulmonary medical image

In the analysis of the number of thoracic pulmonary nodules, the automatic texture extraction of the pulmonary nodules has always been a key issue in traditional algorithms. In the past decades, the manual extraction of the texture morphology of the pulmonary nodules has been the conventional way of designing algorithms.

This section presents an overview of the contribution of deep learning to various application areas in pulmonary medical imaging.

Pulmonary nodule

Lung cancer is one of the most severe cancer types [65]. This disease can be prevented if the pulmonary nodules are detected early and diagnosed correctly. With the help of modern CAD systems, radiologists can detect more pulmonary nodules with much less time [66–69]. Detection, segmentation, and classification of pulmonary nodules are the main functions of the modern CAD system and belong to computer vision, which has achieved huge advance with CNNs (Table 2).

Pulmonary nodule classification

For the classification of pulmonary nodules, most studies focus on how computer-aided detection system provides radiologists with image manifestations, such as type of the nodule (benign or malignant) for the early diagnosis of lung cancer and provides advice for the diagnosis. Fig. 3 provides an illustration of the commonly used classification network.

Owing to the self-learning and generalization ability of deep CNN, it has been applied in the classification of the type of pulmonary nodules. A specific nodule image network structure has been proposed to solve three types of nodule recognition problems, namely, solid, semi-solid, and ground glass opacity (GGO) [70]. Netto *et al.* [71] studied the separation of pulmonary nodule-like structures from other structures, such as blood vessels and bronchi. Finally, the structure is divided into nodules and non-nodules based on shape and texture measurement with support vector machine. Pei *et al.* [72] used a 2D

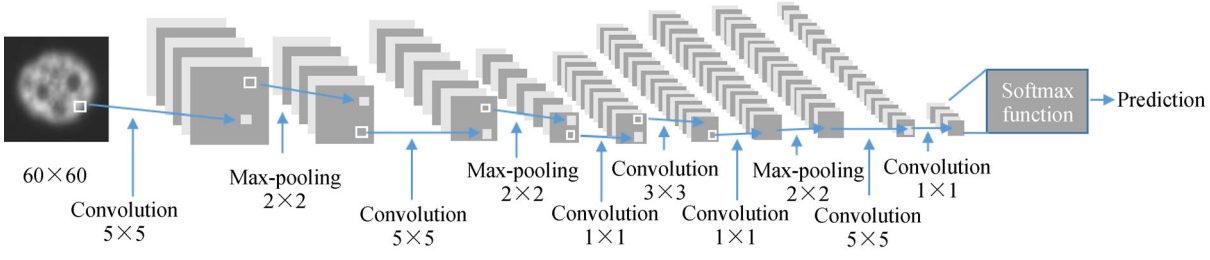

Fig. 3 Structure of classification network. The output are the possibilities of the targets.

Table 2 Deep learning in pulmonary nodule

Authors	Year	Task	Modality	2D/3D	Main methods
Li *et al.* [70]	2016	Nodule type classification	CT	2D	Recognition of three types of nodules
Netto *et al.* [71]	2012	Nodule type classification	CT	3D	The 3D pulmonary nodules were extracted from the lungs (including mediastinum and chest wall), and then classified
Pei *et al.* [72]	2010	Nodule type classification	CT	2D	Geometrically constrained region growth method was used for dividing nodule types
Suzuki *et al.* [73,74]	2005	Benign/malignant classification	LDCT	2D	Distinguished malignant nodules from six different types of benign nodules
Causey *et al.* [75]	2018	Benign/malignant classification	CT	2D, 3D	Compared deep learning and radiomics approaches for lung nodule malignancy prediction
Xie *et al.* [77]	2017	Benign/malignant classification	CT	3D	Proposed a transferable multi-model ensemble algorithm for benign-malignant lung nodule classification on chest CT
Shen *et al.* [78]	2017	Benign/malignant classification	CT	2D, 3D	Cropped different regions from convolutional feature maps and then applied max-pooling different times
Liu *et al.* [79,80]	2018	Benign/malignant classification	CT	2D	Explored the relationship between lung nodule classification and attribute score
Liao *et al.* [81]	2019	Benign/malignant classification	CT	3D	Detected all suspicious lesions (pulmonary nodules) and evaluated the whole-lung/pulmonary malignancy
Ding *et al.* [85]	2017	Nodule detection	CT	3D	Proposed a deconvolutional structure for faster region-based CNN
Winkels *et al.* [86]	2017	Nodule detection	CT	3D	Used 3D roto-translation group convolutions (G-Convs) instead of the more conventional translational convolutions
Zhu *et al.* [87]	2017	Nodule detection	CT	3D	Designed a 3D gaster R-CNN nodule detection with a U-net-like encoder-decoder structure for effectively learning nodule features
Tang *et al.* [88]	2018	Nodule detection	CT	3D	Introduced a novel DCNN approach, consisting of two stages that are fully 3D and end-to-end
Tang *et al.* [89]	2019	Nodule detection	LDCT	3D	Integrated nodule candidate screening and false positive reduction into one model, trained jointly
Xie *et al.* [90]	2018	Nodule detection	CT	3D	Modification of the ResNet and feature pyramid network combined, powered by RReLU activation
Ma *et al.* [91]	2019	Nodule detection	CT	2D, 3D	Used group convolution and attention network to abstract feature and balance the samples with hard negative sample mining
Feng *et al.* [92]	2017	Nodule segmentation	CT	3D	Used weakly supervised method that generates accurate voxel-level nodule segmentation
Messay *et al.* [93]	2015	Nodule segmentation	CT	3D	Used weakly labeled data without dense voxel-level annotations

multi-scale filter for dividing the nodules into nodules and non-nodules by geometrically constrained region growth method.

For benign and malignant classification, Suzuki *et al*. [73,74] developed methods to differentiate benign and malignant nodules in low-density CT scans. Causey *et al*. [75] proposed a method called NoduleX for the prediction of lung nodule malignancy with CT scans. Zhao *et al*. [76] proposed an agile CNN model to overcome the challenges of small-scale medical datasets and nodules. Considering the limited chest CT data, Xie *et al*. [77] used transfer learning algorithm to separate benign and malignant pulmonary nodules. Shen *et al*. [78] presented a multi-crop CNN (MC-CNN) to automatically extract nodule salient information for the investigation of the lung nodule malignancy suspiciousness. Liu *et al*. [79,80] proposed a multi-task model to explore the relatedness between lung nodule classification and the attribute score. Many researchers have used 3D CNNs to predict the malignancy of the pulmonary nodule and achieve a high AUC score [81,82]. Some researchers attempted to make the prediction interpretable by using multitask joint learning [83,84].

Pulmonary nodule detection

The diagnosis of pulmonary nodules is a special detection task. Considering that one pulmonary nodule can go across multi CT slices, most of the existing pulmonary nodule detection methods are based on 3D or 2.5D CNNs (convolution neural networks). The general detection process, including training and testing phases, is illustrated in Fig. 4. A high-performance pulmonary nodule detection system must have high sensitivity and precision. Hence, many researchers have focused on two-stage networks. Two-stage involves one network for nodule candidate detection and the other for false positive reduction (Fig. 5). Ding *et al*. [85] proposed a deconvolutional structure for faster region-based CNN (faster R-CNN) for candidate detection with a 3D DCNN for false positive reduction. A 3D roto-translation group convolution (G-Convs) was introduced for false positive reduction network for improved efficiency and performance [86]. A 3D faster R-CNN with a U-net-like encoder-decoder structure for candidate detection and a gradient boosting machine with a 3D dual path network (DPN) for false positive reduction have been designed [87]. Tang *et al*. [88] used online hard negative mining in the first stage and assembled both stages via consensus until the predictions are realized. Tang *et al*. [89] then proposed an end-to-end method for training the candidate detection and false-positive reduction network together, resulting in improved performance. In pulmonary nodule detection, the imbalanced sample is a severe problem. Two-stage networks use the first stage for choosing positive and hard negative samples, thus providing the second stage with a balanced ratio between positive and negative samples. ResNet [17] and the feature pyramid network combined single stage model have been modified [90]. This model improved the sample imbalance via a patch-based sampling strategy. Another one-stage network based on SSD has been introduced [91]. It uses

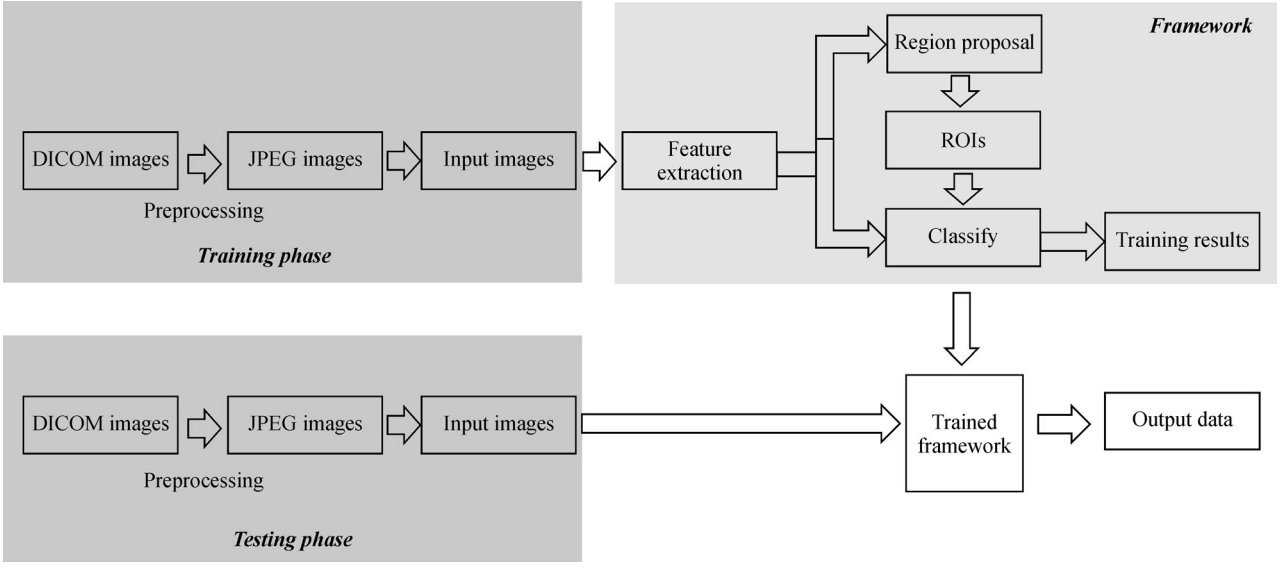

Fig. 4 Illustration of the pipeline for lesion detection. In both training and testing phases, the medical images in DICOM formats are converted and preprocessed to obtain the input images. In the training phase, region proposal methods are used for the extraction of the ROIs of the input images and then adopting classification on the ROIs and output prediction scores. In the testing phase, input images are fed into the trained model generated from the training phase to obtain inference results.

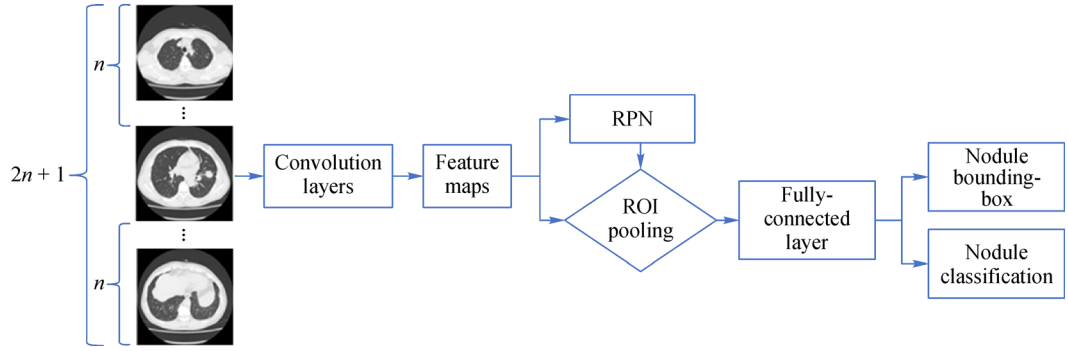

Fig. 5 Structure of the detection network. The region proposal network is used to determine the area candidates of objects, and the subsequent structure serves the function of classification.

group convolution and attention network for abstract features and balances the samples with hard negative sample mining. Liu *et al*. [94] evaluated the influence of radiation dose, patient age, and CT manufacturer on the performance of deep learning applied in nodule detection.

Pulmonary nodule segmentation

Pulmonary nodules are first detected. The segmentation of pulmonary nodules is also important in measuring the size of the nodule, and the malignancy prediction is the final target. The U-net architecture and unsupervised learning are widely adopted in the segmentation task. Considering that the segmentation label is difficult to obtain, a weakly-supervised method that generates accurate voxel-level nodule segmentation has been proposed [102]; this method only needs the image level classification label. Messay *et al*. [103] trained a nodule segmentation model by using weakly labeled data without dense voxel-level annotations.

Pulmonary embolism (PE)

PE is a highly lethal condition that occurs when an artery in the lung becomes partially or completely blocked. It occurs when a thrombus generated from legs, or sometimes other parts of the body, moves to the lungs and obstructs the central, lobar, segmental, or sub-segmental pulmonary arteries depending on the size of the embolus. However, this rate can be decreased to 2%–11% if measures are taken timely and correctly. Although PE is not always fatal, it is the third most threatening disease with at least 650 000 cases occurring annually [104].

CT pulmonary angiography (CTPA) is the primary means for PE diagnosis, wherein a radiologist carefully trace each branch of the pulmonary artery for any suspected PEs. However, in general, CTPA consists of hundreds of images. Each image represent one slice of the lung, and the differentiation of PE with high clinical accuracy is time-consuming and difficult. The diagnosis of PE is a complicated task, because many reasons may result in wrong diagnosis, such as high false-positive results. For instance, respiratory motion, flow-related, streak, partial volume, and stair-step artifacts, lymph nodes, and vascular bifurcation could affect the diagnosis. Thus, computer-aided detection (CAD) is an important tool for radiologists in the detection and diagnosis of PE accurately and decreasing the reading time of CTPA (Table 3).

Matteo Rucco introduced an integrative approach based on Q-analysis with machine learning [95]. The new approach, called Neural Hypernetwork, has been applied in a case study of PE diagnosis, involving data from 28 diagnostic features of 1427 people considered to be at risk

Table 3 Deep learning in PE

Authors	Year	Task	Modality	Main methods
Rucco *et al*. [95]	2015	Classification	X-ray	Introduced an approach for the analysis of partial and incomplete datasets based on Q-analysis
Bi *et al*. [96]	2007	Detection	X-ray	Detected PE from CTPA images
Agharezaei *et al*. [97]	2016	Classification	X-ray	Predicted the risk level of PE
Serpen *et al*. [98]	2008	Classification	X-ray	Used knowledge-based hybrid learning algorithm
Tsai *et al*. [99]	2010	Classification	X-ray	Used GNN network to achieve the PE recognition
Tajbakhsh *et al*. [100]	2015	Classification	X-ray	Investigated the possibility of a unique PE representation
Chen *et al*. [101]	2017	Classification	X-ray	Classified free-text radiology reports

of PE and obtained a satisfying recognition rate of 94%. This study involves a structure-based analysis algorithm. For CTPA image classification, the CAD of PE typically consists of the four following stages: (1) extraction of a volume of interest (VOI) from the original dataset via lung [105–107] or vessel segmentation [108,109], (2) generation of a set of PE candidates within the VOI using algorithms, such as tobogganing [110] and extracting hand-crafted features from each PE candidate [111,112], and (3) computation of a confidence score for each candidate by using a rule-based classifier, neural networks and a nearest neighbor [106,108,113] or multi-instance classifier [110]. Jinbo Bi [96] proposed a new classification method for the automatic detection of PE. Unlike almost all existing PEs search space methods that require vascular segmentation, this method is based on Toboggan's candidate generator, which can quickly and effectively retrieve the suspicious areas of the whole lung. The network provides an effective solution for the learning problem of multiple positive examples to indicate that the action is in progress. The detection sensitivity of 177 clinical cases was 81%.

Nowadays, the neural network method has achieved much attention in PE recognition [114–116]. Scott *et al*. proved that radiologists can improve their interpretations of PE diagnosis by incorporating computer output in formulating diagnostic prediction [117]. Agharezaei *et al*. used the artificial neural network (ANN) for the prediction of the risk level of PE [97]. Serpen *et al*. confirmed that knowledge-based hybrid learning algorithms are configured for providing better performance than the pure empirical mechanical learning algorithms that provide automatic classification tasks associated with medical diagnosis described as PE. A considerable expertise in the PE domain is considered, and the hybrid classifier of knowledge is easily utilized based on both illustration and experience learning [98]. Tsai *et al*. proposed the multiple active contour models, which combine the tree hierarchy to obtain the regional lung and vascular distribution. In the last step of the system, the gabor neural network (GNN) was used to determine the location of the thrombosis. This novel method used the GNN network for recognizing PE, but the accuracy and precision of the results are not good [99]. Tajbakhsh *et al*. investigated the possibility of a unique PE representation, coupled with CNNs, thus increasing the accuracy of PE CAD system for PE CT classification [100]. To eliminate the false-positive detection for the PE recognition, the possibility of implementing neural network as an effective tool for validating CTPA datasets has been investigated [118]. In addition, it improved the accuracy of PE recognition to 83%. Meanwhile, the vessel-aligned multi-planar image representation had three advantages that can improve the PE accuracy. First, the efficiency of the image representation is high, because it is a brief summary of 3D context information near the blockage in two image channels. Second, the image representation consistently supports data enhancement for training the CNN. Therefore, the import extensions can be posted. Third, the image representation is expandable, because it naturally supports data augmentation for training CNN. Besides, Chen *et al*. evaluated the performance of the deep learning CNN model, comparing it with a traditional natural language processing (NLP) model in extracting PE information from the thoracic CT reports from two institutions and proved that the CNN model can classify radiology free-text reports with an accuracy equivalent to or outperform that of an existing traditional NLP model [101].

Pneumonia

Pneumonia is one of the main causes of death among children. Unfortunately, in rural areas in developing countries, infrastructure and medical expertise are lacking for its timely diagnosis. The early diagnosis of interstitial lung disease is essential for treatment. Therefore, chest X-ray examination is one of the most commonly used radiological examinations for the screening and diagnosis of many lung diseases. However, the diagnosis of pneumonia in children by using X-ray is a very difficult task, because the current type of pneumonia image discrimination relies mainly on the experience of doctors. Specialized departments and personnel from hospitals are required for making judgments. This set-up is laborious, and considering that the images of some pneumonia are very similar, doctors can easily make mistake, causing misdiagnoses (Table 4).

Pneumonia usually manifests as one or more opaque areas on the chest radiograph (CXR) [126]. However, the diagnosis of CXR pneumonia is complicated by many other diseases in the lungs, such as fluid overload (pulmonary edema), bleeding, volume loss (atelectasis or collapse), lung cancer, or post-radiation or surgical changes. Generally, medical images are viewed, and a rough estimation of the observed tissue is made to distinguish whether the tissue is normal. In recent decades, the identification of pneumonia has developed rapidly through the computer-assisted technology. The technique pays attention to deep learning. However, many methods are available based on the traditional image pattern recognition. The template matching and learning method based on the statistical mode is one example. Siemens used a template matching algorithm [127] to identify the type of pneumonia. In this work, images were converted from the spatial domain to the frequency domain via Fourier transform infrared spectroscopy, and the target features in the frequency domain were used to classify the pneumonia type. However, the algorithm is computationally intensive and the accuracy is low. A conventional image processing method based on a statistical model can also be used. It

Table 4 Deep learning in pneumonia

Authors	Year	Task	Modality	Main methods
Lee *et al*. [119]	2001	Detection	CT	Used a template matching algorithm for the identification of the type of pneumonia
Abdullah *et al*. [120]	2011	Detection	CT	Proposed a detection method of pneumonia symptoms gray-scale color and the segmentation between normal and lung regions
Correa *et al*. [121]	2018	Classification	Ultrasound	Automatic classification of pneumonia approach based on the analysis of brightness distribution patterns present in rectangular segments
Cisnerosvelarde *et al*. [122]	2016	Detection	Ultrasound	Proposed the application of ultrasound video analysis for the detection of pneumonia
Sharma *et al*. [123]	2017	Detection	X-ray	Used Otsu threshold to segregate the healthy part of lung from the pneumonia infected cloudy regions
de Melo *et al*. [124]	2018	Detection	X-ray	Used parallel technique to improve the computing speed
Wang *et al*. [125]	2017	Classification	X-ray	Built a large-scale and high-accuracy CAD system

generally extracts features manually and then uses a classifier for identification. In general, the modeling is based on the color, texture, shape, and spatial relationship of the image. The algorithms commonly used for texture features are local binary patterns (LBP) mode and direction histograms of oriented gradients (HOG) [128,129].

However, the features extracted by hand cannot accurately distinguish the types of pneumonia. As a recently developed method for the automatic feature extraction, deep learning has been applied to some medical image analysis. The network avoids the complex preprocessing of the images in the early stage and can directly input the images into the network to obtain the recognition results. CNNs can learn the essential characteristics of different pneumonia types autonomously through the convolution kernels. Abdullah *et al*. [120] proposed a detection method for the pneumonia symptoms by using the CNNs based on the difference of gray-scale color and the segmentation between normal and suspicious lung regions. Correa [121,130] introduced a method of automatic diagnosis of pneumonia by pulmonary ultrasound imaging. Different from Refs. [131] and [130], Cisnerosvelarde *et al*. [122] applied pneumonia detection in a new field based on ultrasound videos rather than ultrasound images. To determine an automated diagnostic method for medical images, 40 simulated chest CXRs related to the normal and pneumonia patients were studied [123]. For the detection of pneumonia clouds, the healthy part of the lungs was isolated from the area of pneumonia infection. Then, the algorithm for clipping and extracting lung regions from images was also developed and was compiled based on CUDA [131–133] for an improved computational performance [124].

The scarcity of data and the dependence on the labeled data in the application of deep learning in medical imaging have been analyzed. Wang *et al*. [125] aimed to build a large-scale and high-accuracy CAD system for increased academic interest in building large-scale database of medical images. The author extracted the report contents and tags from the picture archiving and communication system (PACS) of the hospital by NLP and constructed a hospital-scale chest X-ray database.

Tuberculosis

Pulmonary tuberculosis is a chronic infectious disease mainly transmitted by the respiratory tract [35]. Pulmonary tuberculosis is caused by individual factors such as age, genetic factors, and personal behaviors such as smoking and air pollution. Its pathogen is *Mycobacterium tuberculosis*, which can invade the body and cause hematogenous dissemination. At present, the diagnostic methods of tuberculosis mainly depend on historical records, symptoms and signs, imaging diagnosis, and the sputum *Mycobacterium tuberculosis* examination. The chest X-ray examination is an important method for the diagnosis of tuberculosis. It can detect early mild tuberculosis lesions and judge the nature of the lesions.

The success of the method depends on the radiologist's CAD system, which can overcome this problem and accelerate the active case detection (Table 5). In recent years, great progress has been made in the field of deep learning, which allowed the classification of heterogeneous images [134,135]. CNN is popular for its ability to learn intermediate and advanced images. Various CNN models have been used for the classification of CXR into tuberculosis [136]. Lakhani & Sundaram [137] used deep learning with CNNs and achieved accurately classified tuberculosis from the CXR with an area under the curve of 0.99. Melendez *et al*. [138] evaluated the deep learning framework on a database containing 392 patient records with suspected TB subjects. Melendez [139–141] proposed the use of weakly labeled approach for TB detection. It studied an alternative pattern classification method, namely multi-instance learning, which does not require detailed information for training a

Table 5 Deep learning in tuberculosis

Authors	Year	Task	Modality	Main methods
Pande *et al*. [135]	2015	Classification	X-ray	Evaluated the accuracy of CAD software for diagnosis of PTB
Rohilla *et al*. [136]	2017	Classification	X-ray	Used various CNN models to classify the CXR
Lakhani *et al*. [137]	2017	Classification	X-ray	Used deep learning with CNNs and got the accurately classify tuberculosis
Melendez *et al*. [138]	2016	Classification	X-ray	Evaluated this framework on a database containing 392 patient records from suspected TB subjects
Melendez *et al*. [139]	2014	Detection	X-ray	Proposed a method which uses a weakly labeled approach to detect TB
Shin *et al*. [140]	2016	Detection	X-ray	Presented a deep learning model to detect a disease from an image and annotate its contexts
Murphy *et al*. [141]	2019	Detection	X-ray	Automated analysis of chest X-ray (CXR) as a sensitive and inexpensive means of screening susceptible populations for pulmonary tuberculosis
Zheng *et al*. [142]	2017	Detection	X-ray	Found that shallow features or early layers always provide higher detection accuracy
Bar *et al*. [143]	2015	Detection	X-ray	Explored the ability of CNN learned from a nonmedical dataset to identify different types of pathologies in chest X-rays

CAD system. They have applied this alternative method to a CAD system designed for the detection of texture lesions associated with tuberculosis. Then, for solving the problem of having to use additional clinical information in screening for tuberculosis, a combination framework based on machine learning has been proposed [141,145,146]. Zheng *et al*. [142] studied the performance of the known deep convolution network (DCN) structures under different abnormal conditions. In comparison with the deep features, the shallow features or the early layers always provide higher detection accuracy. These techniques have been applied for tuberculosis detection on different datasets and achieved highest accuracy. For classifying abnormalities in the CXRs, a cascade of CNN and recurrent neural network (RNN) have been employed Indiana chest X-rays dataset [140]. However, the accuracy was not compared with previous results. The use of a binary classifier scheme of normal versus abnormal has been attempted [143].

Interstitial lung disease (ILD)

ILD is a group of heterogeneous non-neoplastic and non-infectious lung diseases with alveolar inflammation and interstitial fibrosis as the basic pathological changes. This disease also called diffuse parenchymal lung disease (DPLD). ILD involves several abnormal imaging patterns observed in CT images. The accurate classification of these patterns plays an important role in the accurate clinical judgment of the extent and nature of the disease (Table 6). Therefore, the development of an automatic computer-aided detection system for lung is important.

Anthimopoulos *et al*. [55] proposed and evaluated a CNN for the classification of ILD patterns. This method used the texture classification scheme of the ROI for the generation of an ILD quantization map of the whole lung by sliding a fixed proportion classifier on the pre-segmented lung field. Then, the quantified results were

Table 6 Deep learning in ILD

Authors	Year	Task	Modality	Main methods
Anthimopoulos *et al*. [55]	2016	Classification	CT	Proposed and evaluated a CNN for the classification of ILD patterns
Simonyan and Zisserman [147]	2018	Classification	HRCT	Proposed and developed a framework in which CNN was used for tissue categorization of ILD
Li *et al*. [148]	2013	Classification	HRCT	Used unsupervised algorithm for capturing image features of different scales
Li *et al*. [149]	2014	Classification	HRCT	Proposed a customized CNN architecture to classify HRCT lung image patches of ILD patterns
Gao *et al*. [150]	2016	Classification	CT	Proposed multi-label, multi-class ILD model and trained simultaneously
Christodoulidis *et al*. [151]	2016	Classification	CT	Used multiple transfer of knowledge to improve the accuracy and stability of a CNN on the task of lung tissue pattern classification
Gao *et al*. [152]	2018	Classification	CT	Proved that the use of three attenuation ranges data can enhance the classification effect

used in the final diagnosis of the CAD system. Simonyan and Zisserman [147] developed a CNN framework to classify the lung tissue patterns into different classes such as normal, reticulation, GGO, and honeycombing. Li *et al*. [148] used an unsupervised algorithm to capture image features of different scales and feature extractors of different sizes and achieved a good classification accuracy of 84%. Then, Li *et al*. [149] designed a customized CNN with a shallow convolution layer to classify ILD images. Gao *et al*. [150] proposed two variations of multi-label deep CNNs to accurately recognize the potential multiple ILD co-occurrence on an input lung CT slice. Christodoulidis *et al*. [151] applied algorithms similar to knowledge maps to the classify ILD. In this study, the possibility of transfer learning in the field of medical image analysis and the structural nature of the problem were expressed. The training method of the network is as important as the design of that architecture. By rescaling the original CT images of Hounsfield units to three different scales (one focusing on the low attenuation mode, one focusing on the high attenuation mode, and one focusing on the normal mode), the three 2D images were used as input into the network. Gao *et al*. [152] found that the three attenuation ranges provided a better visibility or visual separation in all six ILD disease categories.

Others

For other pulmonary diseases including common diseases, such as pneumothorax, bullae, and emphysema, deep learning models have many applications, which greatly improve the diagnostic rate of etiology. Cengil *et al*. [153] used deep learning for the classification of cancer types. A semi-supervised deep learning algorithm was proposed to automatically classify patients' lung sounds [154,155] (for the two most common lung sounds, wheezing and bursting). The algorithm made some progress in automatic lung sound recognition and classification. Aykanat *et al*. [156] proposed and implemented a U-net convolution network structure for the biomedical image segmentation. It mainly separates lung regions from the other tissues in the CT images. To facilitate the detection and the classification of lung nodules, Tan *et al*. [157] used a CAD system based on transfer learning (TL) and improved the accuracy of lung disease diagnosis in bronchoscopy. For chronic obstructive pulmonary disease (COPD) [158], the characteristics of long-term short-term memory (LSTM) unit are used for representing the progress of COPD, and a specially configured RNN was used for capturing irregular time-lapse. It improved the explanatory ability of the model and the accuracy of estimating the progress of COPD. Campo *et al*. [159] used X-rays to quantify the emphysema instead of CT scans.

Datasets and performance

Pulmonary nodule datasets

LIDC-IDRI

The Lung Image Database Consortium image collection (LIDC-IDRI) [160] consists of chest medical image files (such as CT and X-ray) and the corresponding pathological markers of the diagnostic results (Table 7). The data were collected by the National Cancer Institute to study early cancer detection in high-risk populations. The dataset contains 1018 research cases, and the nodule diameter in the LIDC-IDRI dataset ranged from 3 mm to 30 mm. For each data, four experienced thoracic radiologists carried out two-stage diagnostic labeling. In the first stage, each radiologist independently examined each CT scan and marked one of three types of lesions ("nodule $\geqslant$ 3 mm," "nodule $<$ 3 mm," and "non-nodule $>$ 3 mm"). On the second phase, each radiologist independently checks his or her own markers and the anonymous markers from three other radiologists to provide final comments. This procedure aims to identify all pulmonary nodules in each CT scan as completely as possible without compulsory consistency. A brief comparison is given in the LIDC-IDRI dataset. Armato *et al*. [161] believed that better results can be obtained by combining geometric texture with the directional gradient histogram with reduced HOG-PCA features to create a hybrid feature vector for each candidate node. Huidrom *et al*. [162] used a nonlinear algorithm to classify the 3D nodule candidate boxes. The proposed algorithm is based on the combination of genetic algorithm (GA) and the particle swarm optimization (PSO) to prove the learning ability of multi-layer perceptron. This method was compared with the existing linear discriminant analysis (LDA) and the convolutional neuron methods. Shaukat *et al*. [163] presented a marker-controlled watershed technique that used intensity, shape, and texture features for the detection of lung nodules. Zhang *et al*. [164] used 3D skeletonization features based on the prior anatomical knowledge for the determination of the lung nodules. Naqi *et al*. [165] used traditional manual feature HOG and CNN features to construct hybrid feature vectors to find candidate nodules. Refs. [166–168] showed algorithms that achieved better results that year. The deep learning methods [71,169–172] for lung nodule detection did not show promising results.

LUNA16

LUNA16 dataset [160,176] is a subset of LIDC-IDRI. LIDC-IDRI that includes 1018 low-dose lung CT images, while LUNA excludes CT images with slices thicker than 3

Table 7 Deep learning in LIDC-IDRI dataset

Authors	Year	Datasets	Main methods	Acc.	Sen.	Spc.	FPs/Scan
Armato *et al*. [161]	2019	LIDC-IDRI	Combined geometric texture with directional gradient histogram with feature reduction of principal component analysis (HOG-PCA) to automatically detect nodules	99.2%	98.3%	98.0%	3.3
Huidrom *et al*. [162]	2019	LIDC-IDRI	Used a nonlinear algorithm to classify the 3D nodule candidate boxes	93.23%	93.26%	93.2%	–
Shaukat *et al*. [163]	2019	LIDC-IDRI	Presented a marker-controlled watershed technique that uses intensity, shape and texture features to detect lung nodules	93.7%	95.5%	94.28%	5.72
Zhang *et al*. [164]	2018	LIDC-IDRI	Used 3D skeletonization feature based prior anatomical knowledge	–	89.3%	–	2.1
Naqi *et al*. [165]	2018	LIDC-IDRI	Used traditional manual feature HOG and CNN feature to construct hybrid feature vectors	98.8%	97.7%	96.2%	3.8
Liu *et al*. [166]	2017	LIDC-IDRI	Presented a fast segmentation method for true nodules and false positive nodules	93.20%	92.40%	94.80%	4.5
Javaid *et al*. [167]	2016	LIDC-IDRI	Extracted 2D and 3D feature sets for nodules to eliminate false positives	96.22%	91.65%	–	3.19
Akram *et al*. [168]	2015	LIDC-IDR	Proposed a novel pulmonary nodule detection technique by thresholding, label masking, background removal and contour correction	97.52%	95.31%	99.73%	–
Dou *et al*. [175]	2016	LUNA16	Used 3D CNNs for false positive reduction	–	90.7%	–	4.0
Setio *et al*. [57]	2016	LUNA16	Used multi-view convolutional networks (ConvNets) to extract the features	–	90.1%	–	4.0

mm and pulmonary nodules smaller than 3 mm. The database is very heterogeneous. It is clinically collected from seven different academic institutions for dose and low-dose CT scans, and it has a wide range of scanner models and acquisition parameters. The final list contains 888 scans. Dou *et al*. [175] employed 3D CNNs for false positive reduction in automated pulmonary nodule detection from volumetric CT scans. Setio *et al*. [57] used multi-view convolutional networks (ConvNets) to extract the features and then combined a dedicated fusion method to obtain the final classification. Other teams [159,161,177] also achieved relatively good results.

Pneumonia datasets

Chest X-ray images

The dataset released by the National Institutes of Health includes 112 120 frontal-view X-ray images of 30 805 unique patients [178]. Fourteen different chest pathological markers were labeled using the NLP method in the *Journal of Radiology*. As a positive example, pneumonia images were identified, and as a negative example of the subject of pneumonia detection, all other images were summarized. The database contains more than 100 000 X-ray front views (about 42 g) of 14 lung diseases (atelectasis, consolidation, infiltration, pneumothorax, edema, emphysema, fibrosis, effusion, pneumonia, pleural thickening, cardiac hypertrophy, nodules, masses, and hernia). Researchers used NLP to label the data. Grades 1 – 14 correspond to 14 kinds of lung diseases, and grade 15 represents 14 kinds of lung diseases. The accuracy of tags in this database exceeded 90%. Wang *et al*. [125] proposed a weakly-supervised multi-label image classification and disease localization framework and achieved F1 score of 0.633. Yao *et al*. [179] used LSTMs to leverage interdependencies among target labels in predicting 14 pathologic patterns and got F1 score of 0.713. Rajpurkar *et al*. [178] improved the result to 0.768 by using a 121-layer DCN (DenseNet).

Tuberculosis datasets

Shenzhen Hospital X-ray

Shenzhen Hospital X-ray [180] is a dataset collected by Shenzhen Third People's Hospital, Guangdong Medical University, Shenzhen, China. Chest X-rays from the clinic were captured as part of the daily hospital routine for a month, mostly in September 2012. This dataset contains 626 frontal chest X-rays, in which 326 are normal, and 336 are accompanied by symptoms of TB. All data were provided in PNG form, which vary in size but are all around 3k $\times$ 3k pixels.

Montgomery County X-ray

The Montgomery County X-ray dataset [180] consists of 138 frontal chest X-rays from the TB screening program in the Department of Health and Human Services, Montgomery County, Maryland, USA. In addition, 80 patients were in normal condition and 58 patients had imaging symptoms of tuberculosis. All pictures were captured using the conventional X-ray machine (cr) to store 12-bit gray level images in the form of portable network graphics (png). They can also be used in the form of DICOM as required. The size of the X-ray is 4020×4892 or 4892×4020 pixels. The work [136] tested deep learning methods on the detection of tuberculosis based on this dataset, and the Shenzhen dataset achieved an accuracy of more than 80% that is comparable performance to the radiologists.

Interstitial lung disease datasets

Geneva database

Geneva database was collected by the University Hospitals of Geneva, Geneva, Switzerland. The dataset consists of chest CT scans of 1266 patients between 2003 and 2008 in the University Hospitals of Geneva. Based on the EHR information, only cases with HRCT (without contrast agent, 1 mm slice thickness) were included. Up until now, more than 700 cases were revised and 128 were stored in the database that affected one of the 13 histological diagnoses of ILDs. The database is available for research on request and after the signature of a license agreement. Anthimopoulos *et al*. [173] and Gangeh *et al*. [174] improved the quantitative measurement of the ILD based on Geneva database.

Challenges and future trends

From the medical and clinical aspects, despite the successes of deep learning technology, many limitations and challenges exist. Deep learning generally requires a large amount of annotated data for analysis. This requirement is a big challenge for annotating medical images. Labeling medical images require expert knowledge, such as the domain knowledge of radiologists. Hence, annotating sufficient medical image is labor- and time-consuming. Although the annotation of medical images is not easy, the amount of unlabeled medical images is vast, because they are well stored in PACS for a long time. If the unlabeled images can be utilized by deep learning techniques, considerable time and effort in annotation would be saved.

Another challenge is the interpretability of deep learning [181]. Deep learning methods are often taken as black box, where their performance or failure is hard to interpret. The demands for the investigation of these techniques increase to pave the way for clinical application of deep learning in medical image analysis. From the perspective of law, the wide spread of deep learning application in medical field would also require transparency and interpretability.

Our future work will further analyze the problem of image semantics segmentation based on the deep learning network, and summarize and improve the shortcomings in the research. Under the background of the research of medical imaging based on deep learning, this paper puts forward several potential or under-study directions in the future. (1) Neural network has a good classification effect on independent and identically distributed test sets, but examples of error classification added to the model, which are not very visually different, will cause a great difference in neural network. Therefore, the Adversarial Net [147] has been proposed to determine a method that can result in higher resolution of medical images based on human eyes. (2) Common methods of machine learning includes supervised learning and unsupervised learning. The current research is based on supervised learning algorithms. However, supervised learning requires human label classification and network training of the data, which can greatly consume the time of medical experts. Senior medical experts often do not have much time to label the training data of a certain order of magnitude. Unsupervised learning may be a potential research direction of medical image processing in the future.

Conclusions

Medical image processing based on deep learning is a hot and challenging subject intersecting the medical field and the computer field. This paper summarizes the research work carried out in the following direction. First, the recent popular DNN framework was introduced, and the origin of its neural network was traced back and discussed in detail. In addition, toward the current deep network framework, the classical models that are universally applied to medical images were introduced.

In the third part of this paper, the application of neural network in various lung diseases was introduced. For the tasks of different diseases, this paper describes the current research status of deep neural network in medical images, analyses and summarizes the development of the framework, and makes a detailed analysis of the models that have achieved good results in these fields to lay an important research foundation for researchers afterwards.

In the fourth part of the article, various algorithm models on datasets such as LIDC-IDRI and LUNA16 were

introduced in detail. In addition, some commonly used datasets on other diseases were briefly introduced in this paper, so that others can carry out relevant experiments.

Compliance with ethics guidelines

Jiechao Ma, Yang Song, Xi Tian, Yiting Hua, Rongguo Zhang, and Jianlin Wu declare that they have no conflicts of interest. This manuscript is a review article that does not need a research protocol requiring approval by the relevant institutional review board or ethics committee.

References

1. LeCun Y, Bengio Y, Hinton G. Deep learning. Nature 2015; 521 (7553): 436–444
2. Schmidhuber J. Deep learning in neural networks: an overview. Neural Netw 2015; 61: 85–117
3. Hosny A, Parmar C, Quackenbush J, Schwartz LH, Aerts HJWL. Artificial intelligence in radiology. Nat Rev Cancer 2018; 18(8): 500–510
4. Camarlinghi N. Automatic detection of lung nodules in computed tomography images: training and validation of algorithms using public research databases. Eur Phys J Plus 2013; 128(9): 110
5. Siegel RL, Miller KD, Jemal A. Cancer Statistics, 2017. CA Cancer J Clin 2017; 67(1): 7–30
6. AbuBaker AA, Qahwaji RS, Aqel MJ, Saleh M. Average row thresholding method for mammogram segmentation. Conf Proc IEEE Eng Med Biol Soc 2005; 3: 3288–3291
7. Haider W, Sharif M, Raza M. Achieving accuracy in early stage tumor identification systems based on image segmentation and 3D structure analysis. Comput Eng Intell Syst 2011; 2(6): 96–102
8. Lo SCB, Lin JS, Freedman MT, *et al*. Computer-assisted diagnosis of lung nodule detection using artificial convoultion neural network[C]//Medical Imaging 1993: Image Processing. International Society for Optics and Photonics. 1993. 1898: 859–869
9. Sahiner B, Chan HP, Petrick N, Wei D, Helvie MA, Adler DD, Goodsitt MM. Classification of mass and normal breast tissue: a convolution neural network classifier with spatial domain and texture images. IEEE Trans Med Imaging 1996; 15(5): 598–610
10. Wang X, Han T X, Yan S. An HOG-LBP human detector with partial occlusion handling[C]//2009 IEEE 12th international conference on computer vision. IEEE. 2009. 32–39
11. Litjens G, Kooi T, Bejnordi BE, Setio AAA, Ciompi F, Ghafoorian M, van der Laak JAWM, van Ginneken B, Sánchez CI. A survey on deep learning in medical image analysis. Med Image Anal 2017; 42: 60–88
12. Zhou H, Yuan Y, Shi C. Object tracking using sift features and mean shift. Comput Vis Image Underst 2009; 113(3): 345–352
13. Mori K, Hahn HK. Computer-aided diagnosis[C]//Proc. of SPIE Vol. 2019. 10950: 1095001–1
14. Russakovsky O, Deng J, Su H, Krause J, Satheesh S, Ma S, Huang Z, Karpathy A, Khosla A, Bernstein M, Berg AC, Fei-Fei L. ImageNet large scale visual recognition challenge. Int J Comput Vis 2015; 115(3): 211–252 (IJCV)
15. Krizhevsky A, Sutskever I, Hinton GE. Imagenet classification with deep convolutional neural networks[C]//Advances in neural information processing systems. 2012. 1097–1105
16. Szegedy C, Liu W, Jia Y, *et al*. Going deeper with convolutions [C]//Proceedings of the IEEE conference on computer vision and pattern recognition. 2015. 1–9
17. He K, Zhang X, Ren S, *et al*. Deep residual learning for image recognition[C]//Proceedings of the IEEE conference on computer vision and pattern recognition. 2016. 770–778
18. Ren S, He K, Girshick R, *et al*. Faster r-cnn: towards real-time object detection with region proposal networks[C]//Advances in neural information processing systems. 2015. 91–99
19. Girshick R. Fast r-cnn[C]//Proceedings of the IEEE international conference on computer vision. 2015. 1440–1448
20. Liu W, Anguelov D, Erhan D, *et al*. Ssd: single shot multibox detector[C]//European conference on computer vision. Springer, Cham. 2016. 21–37
21. Long J, Shelhamer E, Darrell T. Fully convolutional networks for semantic segmentation[C]//Proceedings of the IEEE conference on computer vision and pattern recognition. 2015. 3431–3440
22. Ronneberger O, Fischer P, Brox T. U-net: Convolutional networks for biomedical image segmentation[C]//International Conference on Medical image computing and computer-assisted intervention. Springer, Cham. 2015. 234–241
23. Lederlin M, Revel MP, Khalil A, Ferretti G, Milleron B, Laurent F. Management strategy of pulmonary nodule in 2013. Diagn Interv Imaging 2013; 94(11): 1081–1094
24. Ozekes S, Osman O, Ucan ON. Nodule detection in a lung region that's segmented with using genetic cellular neural networks and 3D template matching with fuzzy rule based thresholding. Korean J Radiol 2008; 9(1): 1–9
25. Shen D, Wu G, Suk HI. Deep learning in medical image analysis. Annu Rev Biomed Eng 2017; 19(1): 221–248
26. Monkam P, Qi S, Ma H, Gao W, Yao Y, Qian W. Detection and classification of pulmonary nodules using convolutional neural networks: a survey. IEEE Access 2019; 7: 78075–78091
27. Wall B, Hart D. Revised radiation doses for typical X-ray examinations. Report on a recent review of doses to patients from medical X-ray examinations in the UK by NRPB. National Radiological Protection Board.. Br J Radiol 1997; 70(833): 437–439

28. Ashby WR. An introduction to cybernetics. Chapman & Hall Ltd, 1961
29. Wiener N. Cybernetics. Bull Am Acad Arts Sci 1950; 3(7): 2–4
30. Rosenblatt F. The perceptron: a probabilistic model for information storage and organization in the brain. Psychol Rev 1958; 65(6): 386–408
31. Hubel DH, Wiesel TN. Receptive fields, binocular interaction and functional architecture in the cat's visual cortex. J Physiol 1962; 160(1): 106–154
32. Rodieck RW, Stone J. Analysis of receptive fields of cat retinal ganglion cells. J Neurophysiol 1965; 28(5): 833–849
33. Blakemore C. The working brain. Nature 1972; 239(5373): 473
34. Fukushima K. Neocognitron: a self organizing neural network model for a mechanism of pattern recognition unaffected by shift in position. Biol Cybern 1980; 36(4): 193–202
35. Fukushima K, Hirota M, Terasaki PI, Wakisaka A, Togashi H, Chia D, Suyama N, Fukushi Y, Nudelman E, Hakomori S. Characterization of sialosylated Lewisx as a new tumor-associated antigen. Cancer Res 1984; 44(11): 5279–5285
36. Fukushima K, Miyake S, Ito T. Neocognitron: a neural network model for a mechanism of visual pattern recognition. IEEE Trans Syst Man Cybern 1983 (5): 826–834
37. Rumelhart DE, Hinton GE, Williams RJ. Learning representations by back-propagating errors. Nature 1988; 323(6088): 696–699
38. Nitta T. Solving the XOR problem and the detection of symmetry using a single complex-valued neuron. Neural Netw 2003; 16(8): 1101–1105
39. Pineda FJ. Generalization of back-propagation to recurrent neural networks. Phys Rev Lett 1987; 59(19): 2229–2232
40. Wigner EP. The problem of measurement. Am J Phys 1963; 31(1): 6–15
41. Hecht-Nielsen R. Theory of the backpropagation neural network. Neural Netw 1988; 1: 445–448
42. Rumelhart DE, Hinton GE, Williams RJ. Learning representations by back-propagating errors. Nature 1988; 323(6088): 696–699
43. LeCun Y. Generalization and network design strategies. Connectionism in perspective. Amsterdam: Elsevier, 1989.Vol. 19
44. LeCun Y, Bottou L, Bengio Y, Haffner P. Gradient-based learning applied to document recognition. Proc IEEE 1998; 86(11): 2278–2324
45. Hinton GE, Osindero S, Teh YW. A fast learning algorithm for deep belief nets. Neural Comput 2006; 18(7): 1527–1554
46. Krizhevsky A, Sutskever I, Hinton GE. Imagenet classification with deep convolutional neural networks. In: Advances in neural information processing systems. 2012. 1097–1105
47. Simonyan K, Zisserman A. Very deep convolutional networks for large-scale image recognition. arXiv preprint. 2014. arXiv: 1409.1556
48. Huang G, Liu Z, Van Der Maaten L, Weinberger KQ. Densely connected convolutional networks. In: Proceedings of the IEEE conference on computer vision and pattern recognition. 2017. 4700–4708
49. Krogh A, Hertz JA. Dynamics of generalization in linear perceptrons. In: Advances in Neural Information Processing Systems. 1991. 897–903
50. LeCun Y, Boser B E, Denker JS, Henderson D, Howard RE, Hubbard WE, Jackel LD. Handwritten digit recognition with a back-propagation network. In: Advances in neural information processing systems. 1990. 396–404
51. Haskell BG, Howard PG, LeCun YA, Puri A, Ostermann J, Civanlar MR, Rabiner L, Bottou L, Haffner P. Image and video coding-emerging standards and beyond. IEEE Trans Circ Syst Video Tech 1998; 8(7): 814–837
52. Hochreiter S, Bengio Y, Frasconi P, Schmidhuber J. Gradient flow in recurrent nets: the difficulty of learning long-term dependencies. 2001
53. Pedrazzi M, Patrone M, Passalacqua M, Ranzato E, Colamassaro D, Sparatore B, Pontremoli S, Melloni E. Selective proinflammatory activation of astrocytes by high-mobility group box 1 protein signaling. J Immunol 2007; 179(12): 8525–8532
54. Deng J, Dong W, Socher R, Li LJ, Li K, Li FF. Imagenet: a large-scale hierarchical image database. In: 2009 IEEE conference on computer vision and pattern recognition. 2009. 248–255
55. Anthimopoulos M, Christodoulidis S, Ebner L, Christe A, Mougiakakou S. Lung pattern classification for interstitial lung diseases using a deep convolutional neural network. IEEE Trans Med Imaging 2016; 35(5): 1207–1216
56. Kawahara J, BenTaieb A, Hamarneh G. Deep features to classify skin lesions. In: 2016 IEEE 13th International Symposium on Biomedical Imaging (ISBI). 2016. 1397–1400
57. Setio AAA, Ciompi F, Litjens G, Gerke P, Jacobs C, van Riel SJ, Wille MMW, Naqibullah M, Sanchez CI, van Ginneken B. Pulmonary nodule detection in CT images: false positive reduction using multi-view convolutional networks. IEEE Trans Med Imaging 2016; 35(5): 1160–1169
58. Yang D, Zhang S, Yan Z, Tan C, Li K, Metaxas D. Automated anatomical landmark detection ondistal femur surface using convolutional neural network. In: Biomedical Imaging (ISBI), 2015 IEEE 12th International Symposium on. 2015. 17–21
59. de Vos BD, Wolterink JM, de Jong PA, Viergever MA, Išgum I. 2D image classification for 3D anatomy localization: employing deep convolutional neural networks. In: Medical Imaging 2016: Image Processing. 2016. vol. 9784, p. 97841Y
60. Zheng Y, Liu D, Georgescu B, Nguyen H, Comaniciu D. 3D deep learning for efficient and robust landmark detection in volumetric data. In: International Conference on Medical Image Computing and Computer-Assisted Intervention. Springer. 2015. 565–572
61. Ronneberger O, Fischer P, Brox T. U-net: convolutional networks for biomedical image segmentation. In: International Conference on Medical image computing and computer-assisted intervention. Springer. 2015. 234–241
62. Long J, Shelhamer E, Darrell T. Fully convolutional networks for semantic segmentation. In: Proceedings of the IEEE conference on computer vision and pattern recognition. 2015. 3431–3440
63. Cicek O, Abdulkadir A, Lienkamp SS, Brox T, Ronneberger O. 3D U-Net: learning dense volumetric segmentation from sparse annotation. In: International Conference on Medical Image Computing and Computer-Assisted Intervention. Springer. 2016. 424–432
64. Milletari F, Navab N, Ahmadi SA. V-net: fully convolutional neural networks for volumetric medical image segmentation. In: 2016 Fourth International Conference on 3D Vision (3DV). 565–571
65. Siegel RL, Miller KD, Jemal A. Cancer statistics, 2018. CA Cancer

J Clin 2018; 68(1): 7–30

66. Awai K, Murao K, Ozawa A, Komi M, Hayakawa H, Hori S, Nishimura Y. Pulmonary nodules at chest CT: effect of computer-aided diagnosis on radiologists' detection performance. Radiology 2004; 230(2): 347–352
67. Ciompi F, Chung K, van Riel SJ, Setio AAA, Gerke PK, Jacobs C, Scholten ET, Schaefer-Prokop C, Wille MMW, Marchianò A, Pastorino U, Prokop M, van Ginneken B. Towards automatic pulmonary nodule management in lung cancer screening with deep learning. Sci Rep 2017; 7(1): 46479
68. Liu S, Xie Y, Jirapatnakul A, Reeves AP. Pulmonary nodule classification in lung cancer screening with three-dimensional convolutional neural networks. J Med Imaging (Bellingham) 2017; 4(4): 041308
69. Hua KL, Hsu CH, Hidayati SC, Cheng WH, Chen YJ. Computer-aided classification of lung nodules on computed tomography images via deep learning technique. Onco Targets Ther 2015; 8: 2015–2022
70. Li W, Cao P, Zhao D, Wang J. Pulmonary nodule classification with deep convolutional neural networks on computed tomography images. Comput Math Methods Med 2016; 2016: 6215085
71. Magalhães Barros Netto S, Corrêa Silva A, Acatauassú Nunes R, Gattass M. Automatic segmentation of lung nodules with growing neural gas and support vector machine. Comput Biol Med 2012; 42(11): 1110–1121
72. Pei X, Guo H, Dai J. Computerized detection of lung nodules in CT images by use of multiscale filters and geometrical constraint region growing[C]//2010 4th International Conference on Bioinformatics and Biomedical Engineering. IEEE. 2010: 1–4
73. Suzuki K, Li F, Sone S, Doi K. Computer-aided diagnostic scheme for distinction between benign and malignant nodules in thoracic low-dose CT by use of massive training artificial neural network. IEEE Trans Med Imaging 2005; 24(9): 1138–1150
74. Suzuki K, Doi K. Computerized scheme for distinction between benign and malignant nodules in thoracic low-dose CT: U.S. Patent Application 11/181,884[P]. 2006-1-26
75. Causey JL, Zhang J, Ma S, Jiang B, Qualls JA, Politte DG, Prior F, Zhang S, Huang X. Highly accurate model for prediction of lung nodule malignancy with CT scans. Sci Rep 2018; 8(1): 9286
76. Zhao X, Liu L, Qi S, Teng Y, Li J, Qian W. Agile convolutional neural network for pulmonary nodule classification using CT images. Int J CARS 2018; 13(4): 585–595
77. Xie Y, Xia Y, Zhang J, *et al*. Transferable multi-model ensemble for benign-malignant lung nodule classification on chest CT[C]// International Conference on Medical Image Computing and Computer-Assisted Intervention. Springer, Cham, 2017. 656–664
78. Shen W, Zhou M, Yang F, Yu D, Dong D, Yang C, Zang Y, Tian J. Multi-crop convolutional neural networks for lung nodule malignancy suspiciousness classification. Pattern Recognit 2017; 61: 663–673
79. Liu L, Dou Q, Chen H, Olatunji IE, Qin J, Heng PA. Mtmr-net: Multi-task deep learning with margin ranking loss for lung nodule analysis. In: Deep Learning in Medical Image Analysis and Multimodal Learning for Clinical Decision Support. Springer. 2018. 74–82
80. Heng PA. Mtmr-net: Multi-task deep learning with margin ranking loss for lung nodule analysis. In: Deep Learning in Medical Image Analysis and Multimodal Learning for Clinical Decision Support: 4th International Workshop, DLMIA 2018, and 8th International Workshop, ML-CDS 2018, Held in Conjunction with MICCAI 2018, Granada, Spain, September 20, 2018, Proceedings. 2018. vol. 11045, p. 74
81. Liao F, Liang M, Li Z, Hu X, Song S. Evaluate the malignancy of pulmonary nodules using the 3D deep leaky noisy-or network. IEEE Trans Neural Netw Learn Syst 2019; 1–12
82. Ardila D, Kiraly AP, Bharadwaj S, Choi B, Reicher JJ, Peng L, Tse D, Etemadi M, Ye W, Corrado G, Naidich DP, Shetty S. End-to-end lung cancer screening with three-dimensional deep learning on low-dose chest computed tomography. Nat Med 2019; 25(6): 954–961
83. Wu B, Zhou Z, Wang J, Wang Y. Joint learning for pulmonary nodule segmentation, attributes and malignancy prediction. In: 2018 IEEE 15th International Symposium on Biomedical Imaging (ISBI 2018). 2018. 1109–1113
84. Shen S, Han SX, Aberle DR, Bui AAT, Hsu W. An interpretable deep hierarchical semantic convolutional neural network for lung nodule malignancy classification. Expert Syst Appl 2019; 128: 84–95
85. Ding J, Li A, Hu Z, Wang L. Accurate pulmonary nodule detection in computed tomography images using deep convolutional neural networks. Medical Image Computing and Computer Assisted Intervention – MICCAI 2017. 2017. Springer. 559–567
86. Winkels M, Cohen T S. 3D g-cnns for pulmonary nodule detection. arXiv preprint. 2018. arXiv:1804.04656
87. Zhu W, Liu C, Fan W, Xie X. Deeplung: 3D deep convolutional nets for automated pulmonary nodule detection and classification. arXiv preprint. 2017. arXiv:1709.05538
88. Tang H, Kim DR, Xie X. Automated pulmonary nodule detection using 3D deep convolutional neural networks. International Symposium on Biomedical Imaging. 2018. 523–526
89. Tang H, Liu XW, Xie XH. An end-to-end framework for integrated pulmonary nodule detection and false positive reduction. arXiv preprint. 2019. arXiv:1903.09880
90. Xie Z. Towards single-phase single-stage detection of pulmonary nodules in chest CT imaging. arXiv preprint. 2018. arXiv: 1807.05972
91. Ma JC, *et al*. Group-Attention Single-Shot Detector (GA-SSD): finding pulmonary nodules in large-scale CT images. arXiv preprint. 2018. arXiv:1812.07166
92. Feng X, Yang J, Laine AF, Angelini ED. Discriminative localization in cnns for weakly-supervised segmentation of pulmonary nodules. Medical image computing and computer assisted intervention. 2017. 568–576
93. Messay T, Hardie RC, Tuinstra TR. Segmentation of pulmonary nodules in computed tomography using a regression neural network approach and its application to the Lung Image Database Consortium and Image Database Resource Initiative dataset. Med Image Anal 2015; 22(1): 48–62
94. Liu K, Li Q, Ma J, Zhou Z, Sun M, Deng Y, Xiao Y. Evaluating a fully automated pulmonary nodule detection approach and its impact on radiologist performance. Radiol Artif Intell 2019. 1(3): e180084
95. Rucco M, Sousa-Rodrigues D, Merelli E, Johnson JH, Falsetti L, Nitti C, Salvi A. Neural hypernetwork approach for pulmonary

embolism diagnosis. BMC Res Notes 2015; 8(1): 617
96. Bi J, Liang J. Multiple instance learning of pulmonary embolism detection with geodesic distance along vascular structure. 2007 IEEE Conference on Computer Vision and Pattern Recognition. 2007. 1–8
97. Agharezaei L, Agharezaei Z, Nemati A, Bahaadinbeigy K, Keynia F, Baneshi MR, Iranpour A, Agharezaei M. The prediction of the risk level of pulmonary embolism and deep vein thrombosis through artificial neural network. Acta Inform Med 2016; 24(5): 354–359
98. Serpen G, Tekkedil DK, Orra M. A knowledge-based artificial neural network classifier for pulmonary embolism diagnosis. Comput Biol Med 2008; 38(2): 204–220
99. Tsai H, Chin C, Cheng Y. Intelligent pulmonary embolsim detection system. Biomed Eng (Singapore) 2012; 24(6): 471–483
100. Tajbakhsh N, Gotway MB, Liang J. Computer-aided pulmonary embolism detection using a novel vessel-aligned multi-planar image representation and convolutional neural networks. MICCAI 2015: Medical Image Computing and Computer-Assisted Intervention. 2015. 62–69
101. Chen MC, Ball RL, Yang L, Moradzadeh N, Chapman BE, Larson DB, Langlotz CP, Amrhein TJ, Lungren MP. Deep learning to classify radiology free-text reports. Radiology 2017; 286(3): 845–852
102. Rumelhart DE, Hinton GE, Williams RJ. Learning representations by back-propagating errors. Nature 1988; 323(6088): 696–699
103. Messay T, Hardie RC, Tuinstra TR. Segmentation of pulmonary nodules in computed tomography using a regression neural network approach and its application to the Lung Image Database Consortium and Image Database Resource Initiative dataset. Med Image Anal 2015; 22(1): 48–62
104. Breiman L. Bagging predictors. Mach Learn 1996; 24(2): 123–140
105. Blackmon KN, Florin C, Bogoni L, McCain JW, Koonce JD, Lee H, Bastarrika G, Thilo C, Costello P, Salganicoff M, Joseph Schoepf U. Computer-aided detection of pulmonary embolism at CT pulmonary angiography: can it improve performance of inexperienced readers? Eur Radiol 2011; 21(6): 1214–1223
106. Wang X, Song X F, Chapman B E, *et al*. Improving performance of computer-aided detection of pulmonary embolisms by incorporating a new pulmonary vascular-tree segmentation algorithm[C]// Medical Imaging 2012: Computer-Aided Diagnosis. International Society for Optics and Photonics. 2012. 8315: 83152U
107. Loud PA, Katz DS, Bruce DA, Klippenstein DL, Grossman ZD. Deep venous thrombosis with suspected pulmonary embolism: detection with combined CT venography and pulmonary angiography. Radiology 2001; 219(2): 498–502
108. Özkan H, Osman O, Şahin S, Boz AF. A novel method for pulmonary embolism detection in CTA images. Comput Methods Programs Biomed 2014; 113(3): 757–766
109. Schoepf UJ, Costello P. CT angiography for diagnosis of pulmonary embolism: state of the art. Radiology 2004; 230(2): 329–337
110. Liang J, Bi J. Computer aided detection of pulmonary embolism with tobogganing and mutiple instance classification in CT pulmonary angiography. In: Biennial International Conference on Information Processing in Medical Imaging. Springer. 2007. 630–641
111. Engelke C, Schmidt S, Bakai A, Auer F, Marten K. Computer-assisted detection of pulmonary embolism: performance evaluation in consensus with experienced and inexperienced chest radiologists. Eur Radiol 2008; 18(2): 298–307
112. Liang J, Bi J. Local characteristic features for computer-aided detection of pulmonary embolism in CT angiography. In: Proceedings of the First MICCAI Workshop on Pulmonary Image Analysis. 2008. 263–272
113. Park SC, Chapman BE, Zheng B. A multistage approach to improve performance of computer-aided detection of pulmonary embolisms depicted on CT images: preliminary investigation. IEEE Trans Biomed Eng 2011; 58(6): 1519–1527
114. Tajbakhsh N, Shin JY, Gurudu SR, Hurst RT, Kendall CB, Gotway MB, Liang JM. Convolutional neural networks for medical image analysis: Full training or fine tuning? IEEE Trans Med Imaging 2016; 35(5): 1299–1312
115. Tang L, Wang L, Pan S, Su Y, Chen Y. A neural network to pulmonary embolism aided diagnosis with a feature selection approach. 2010 3rd International Conference on Biomedical Engineering and Informatics. IEEE. 2010. 2255–2260
116. Ebrahimdoost Y, Dehmeshki J, Ellis TS, Firoozbakht M, Youannic A, Qanadli SD. Medical image segmentation using active contours and a level set model: application to pulmonary embolism (PE) segmentation. 2010 Fourth International Conference on Digital Society. IEEE. 2010. 269–273
117. Scott JA, Palmer EL, Fischman AJ. How well can radiologists using neural network software diagnose pulmonary embolism? AJR Am J Roentgenol 2000; 175(2): 399–405
118. Tajbakhsh N, Gotway MB, Liang J. Computer-aided pulmonary embolism detection using a novel vesselaligned multi-planar image representation and convolutional neural networks. In: International Conference on Medical Image Computing and Computer-Assisted Intervention. Springer. 2015. 62–69
119. Lee Y, Hara T, Fujita H, Itoh S, Ishigaki T. Automated detection of pulmonary nodules in helical CT images based on an improved template-matching technique. IEEE Trans Med Imaging 2001; 20 (7): 595–604
120. Abdullah AA, Posdzi NM, Nishio Y. Preliminary study of pneumonia symptoms detection method using cellular neural network. In: International Conference on Electrical, Control and Computer Engineering 2011 (InECCE). 2011. 497–500
121. Correa M, Zimic M, Barrientos F, Barrientos R, Román-Gonzalez A, Pajuelo MJ, Anticona C, Mayta H, Alva A, Solis-Vasquez L, Figueroa DA, Chavez MA, Lavarello R, Castañeda B, Paz-Soldán VA, Checkley W, Gilman RH, Oberhelman R. Automatic classification of pediatric pneumonia based on lung ultrasound pattern recognition. PLoS One 2018; 13(12): e0206410
122. Cisnerosvelarde P, Correa M, Mayta H, Anticona C, Pajuelo M, Oberhelman RA, Checkley W, Gilman RH, Figueroa D, Zimic M, *et al*. Automatic pneumonia detection based on ultrasound video analysis. 2016 38th Annual International Conference of the IEEE Engineering in Medicine and Biology Society (EMBC). IEEE. 2016. 4117–4120
123. Sharma A, Raju D, Ranjan S. Detection of pneumonia clouds in chest X-ray using image processing approach[C]//2017 Nirma University International Conference on Engineering (NUiCONE). IEEE. 2017. 1–4

124. de Melo G, Macedo S O, Vieira S L, *et al*. Classification of images and enhancement of performance using parallel algorithm to detection of pneumonia. 2018 IEEE International Conference on Automation/XXIII Congress of the Chilean Association of Automatic Control (ICA-ACCA). IEEE. 2018. 1–5
125. Wang X, Peng Y, Lu L, Lu Z, Bagheri M, Summers RM. Chestx-ray8: hospital-scale chest X-ray database and benchmarks on weakly-supervised classification and localization of common thorax diseases. The IEEE Conference on Computer Vision and Pattern Recognition (CVPR). 2017. 3462–3471
126. Franquet T. Imaging of community-acquired pneumonia. J Thorac Imaging 2018; 33(5): 282–294
127. Lee Y, Hara T, Fujita H, Itoh S, Ishigaki T. Automated detection of pulmonary nodules in helical CT images based on an improved template-matching technique. IEEE Trans Med Imaging 2001; 20(7): 595–604
128. Nanni L, Lumini A, Brahnam S. Local binary patterns variants as texture descriptors for medical image analysis. Artif Intell Med 2010; 49(2): 117–125
129. Dalal N, Triggs B. Histograms of oriented gradients for human detection. Proceedings of the 2005 IEEE Computer Society Conference on Computer Vision and Pattern Recognition (CVPR'05). 2005. 886–893
130. Barrientos R, Roman-Gonzalez A, Barrientos F, *et al*. Automatic detection of pneumonia analyzing ultrasound digital images. 2016 IEEE 36th Central American and Panama Convention. 2016. 1–4
131. Nvidia C. Nvidia cuda c programming guide. Nvidia Corporation 2011; 120(18): 8
132. Dye C. Global epidemiology of tuberculosis. Lancet 2006; 367 (9514): 938–940
133. Sudre P, ten Dam G, Kochi A. Tuberculosis: a global overview of the situation today. Bull World Health Organ 1992; 70(2): 149–159
134. Ponnudurai N, Denkinger C M, Van Gemert W, *et al*. New TB tools need to be affordable in the private sector: The case study of Xpert MTB/RIF. J Epidemiol Glob Health 2018; 8(3–4): 103–105
135. Pande T, Cohen C, Pai M, Ahmad Khan F. Computer aided diagnosis of tuberculosis using digital chest radiographs: a systematic review. Chest 2015; 148(4 Suppl): 135A
136. Rohilla A, Hooda R, Mittal A. Tb detection in chest radiograph using deep learning architecture. ICETETSM-17. 2017. 136–147
137. Lakhani P, Sundaram B. Deep learning at chest radiography: automated classification of pulmonary tuberculosis by using convolutional neural networks. Radiology 2017; 284(2): 574–582
138. Melendez J, Sánchez CI, Philipsen RHHM, Maduskar P, Dawson R, Theron G, Dheda K, van Ginneken B. An automated tuberculosis screening strategy combining X-ray-based computer-aided detection and clinical information. Sci Rep 2016; 6(1): 25265
139. Melendez J, Sánchez CI, Philipsen RHHM, *et al*. Multiple-instance learning for computer-aided detection of tuberculosis. Computer-Aided Diagnosis. International Society for Optics and Photonics. 2014. 9035: 90351J
140. Shin HC, Roberts K, Lu L, Demner-Fushman D, Yao J, Summers RM. Learning to read chest X-rays: recurrent neural cascade model for automated image annotation. Proceedings of the IEEE conference on computer vision and pattern recognition. 2016. 2497–2506
141. Murphy K, Habib S S, Zaidi S M A, *et al*. Computer aided detection of tuberculosis on chest radiographs: an evaluation of the CAD4TB v6 system. arXiv preprint. 2019. arXiv:1903.03349
142. Zheng Y, Liu D, Georgescu B, Nguyen H, Comaniciu D. 3D deep learning for efficient and robust landmark detection in volumetric data. International Conference on Medical Image Computing and Computer-Assisted Intervention. 2015. 565–572
143. Bar Y, Diamant I, Wolf L, Lieberman S, Konen E, Greenspan H. Chest pathology detection using deep learning with non-medical training. 2015 IEEE 12th International Symposium on Biomedical Imaging (ISBI). 2015. 294–297
144. Feng X, Yang J, Laine AF, Angelini ED. Discriminative Localization in CNNs for Weakly-Supervised Segmentation of Pulmonary Nodules. Medical Image Computing and Computer Assisted Intervention – MICCAI 2017. Springer. 2017. 568–576
145. Melendez J, van Ginneken B, Maduskar P, Philipsen RHHM, Reither K, Breuninger M, Adetifa IMO, Maane R, Ayles H, Sánchez CI. A novel multiple-instance learning-based approach to computer-aided detection of tuberculosis on chest X-rays. IEEE Trans Med Imaging 2015; 34(1): 179–192
146. Melendez J, Sánchez CI, Philipsen RH, Maduskar P, Dawson R, Theron G, Dheda K, van Ginneken B. An automated tuberculosis screening strategy combining X-ray-based computer-aided detection and clinical information. Sci Rep 2016; 6(1): 25265
147. Simonyan K, Zisserman A. Very deep convolutional networks for large-scale image recognition. Computer Vision and Pattern Recognition. arXiv preprint. 2014. arXiv:1409.1556
148. Li Q, Cai W, Feng DD. Lung image patch classification with automatic feature learning. 2013 35th Annual International Conference of the IEEE Engineering in Medicine and Biology Society (EMBC). IEEE. 2013. 6079–6082
149. Li Q, Cai W, Wang X, Zhou Y, Feng DD, Chen M. Medical image classification with convolutional neural network. 13th International Conference on Control Automation Robotics & Vision (ICARCV). IEEE. 2014. 844–848
150. Gao M, Xu Z, Lu L, *et al*. Multi-label deep regression and unordered pooling for holistic interstitial lung disease pattern detection[C]//International Workshop on Machine Learning in Medical Imaging. Springer, Cham. 2016.147–155
151. Christodoulidis S, Anthimopoulos M, Ebner L, Christe A, Mougiakakou S. Multisource transfer learning with convolutional neural networks for lung pattern analysis. IEEE J Biomed Health Inform 2017; 21(1): 76–84
152. Gao M, Bagci U, Lu L, Wu A, Buty M, Shin HC, Roth H, Papadakis GZ, Depeursinge A, Summers RM, Xu Z, Mollura DJ. Holistic classification of CT attenuation patterns for interstitial lung diseases via deep convolutional neural networks. Comput Methods Biomech Biomed Eng Imaging Vis 2018; 6(1): 1–6
153. Cengil E, Çinar A. A deep learning based approach to lung cancer identification[C]//2018 International Conference on Artificial Intelligence and Data Processing (IDAP). IEEE. 2018. 1–5
154. Chamberlain D, Kodgule R, Ganelin D, Miglani V, Fletcher R. Application of semi-supervised deep learning to lung sound analysis. 2016 38th Annual International Conference of the IEEE Engineering in Medicine and Biology Society (EMBC). IEEE.

2016. 804–807
155. Hashemi A, Arabalibiek H, Agin K. Classification of wheeze sounds using wavelets and neural networks. In: 2011 International Conference on Biomedical Engineering and Technology. Singapore: IACSIT Press. 2011. vol. 11. 127–131
156. Aykanat M, Kılıç Ö, Kurt B, Saryal S. Classification of lung sounds using convolutional neural networks. EURASIP J Image Video Processing 2017; 2017: 65
157. Tan T, Li Z, Liu H, Zanjani FG, Ouyang Q, Tang Y, Hu Z, Li Q. Optimize transfer learning for lung diseases in bronchoscopy using a new concept: sequential fine-tuning. IEEE J Transl Eng Health Med 2018; 6: 1800808
158. Tang C, Plasek JM, Zhang H, Xiong Y, Bates DW, Zhou L. A deep learning approach to handling temporal variation in chronic obstructive pulmonary disease progression. 2018 IEEE International Conference on Bioinformatics and Biomedicine (BIBM). IEEE. 2018. 502–509
159. Campo MI, Pascau J, Estepar RSJ. Emphysema quantification on simulated X-rays through deep learning techniques. 2018 IEEE 15th International Symposium on Biomedical Imaging (ISBI 2018). IEEE. 2018. 273–276
160. Armato III SG, McLennan G, Bidaut L, *et al*. The lung image database consortium (LIDC) and image database resource initiative (IDRI): a completed reference database of lung nodules on CT scans. Med Phys 2011; 38(2): 915–931
161. Armato SG 3rd, Giger ML, Moran CJ, Blackburn JT, Doi K, MacMahon H. Computerized detection of pulmonary nodules on CT scans. Radiographics 1999; 19(5): 1303–1311
162. Huidrom R, Chanu YJ, Singh KM. Pulmonary nodule detection on computed tomography using neuroevolutionary scheme. Signal Image Video Process 2019; 13(1): 53–60
163. Shaukat F, Raja G, Ashraf R, Khalid S, Ahmad M, Ali A. Artificial neural network based classification of lung nodules in CT images using intensity, shape and texture features. J Ambient Intell Humaniz Comput 2019; 10(10): 4135–4149
164. Zhang W, Wang X, Li X, Chen J. 3D skeletonization feature based computer-aided detection system for pulmonary nodules in CT datasets. Comput Biol Med 2018; 92: 64–72
165. Naqi S, Sharif M, Yasmin M, Fernandes SL. Lung nodule detection using polygon approximation and hybrid features from CT images. Curr Med Imaging Rev 2018; 14(1): 108–117
166. Liu JK, Jiang HY, Gao MD, He CG, Wang Y, Wang P, Ma H, Li Y. An assisted diagnosis system for detection of early pulmonary nodule in computed tomography images. J Med Syst 2017; 41(2): 30
167. Javaid M, Javid M, Rehman MZU, Shah SIA. A novel approach to CAD system for the detection of lung nodules in CT images. Comput Methods Programs Biomed 2016; 135: 125–139
168. Akram S, Javed MY, Akram MU, Qamar U, Hassan A. Pulmonary nodules detection and classification using hybrid features from computerized tomographic images. J Med Imaging Health Inform 2016; 6(1): 252–259
169. Özkan H, Osman O, Şahin S, Boz AF. A novel method for pulmonary embolism detection in CTA images. Comput Methods Programs Biomed 2014; 113(3): 757–766
170. Mehre S A, Mukhopadhyay S, Dutta A, *et al*. An automated lung nodule detection system for CT images using synthetic minority oversampling[C]//Medical Imaging 2016: Computer-Aided Diagnosis. International Society for Optics and Photonics. 2016. 9785: 97850H
171. Naqi SM, Sharif M, Lali IU. A 3D nodule candidate detection method supported by hybrid features to reduce false positives in lung nodule detection. Multimedia Tools Appl 2019; 78(18): 26287–26311
172. Huidrom R, Chanu YJ, Singh KM. Pulmonary nodule detection on computed tomography using neuroevolutionary scheme. Signal Image Video Process 2019; 13(1): 53–60
173. Anthimopoulos M, Christodoulidis S, Christe A, Mougiakako S. Classification of interstitial lung disease patterns using local DCT features and random forest. 2014 36th Annual International Conference of the IEEE Engineering in Medicine and Biology Society. 2014. 6040–6043
174. Gangeh MJ, Sorensen L, Shaker SB, Kamel MS, de Bruijne M, Loog M. A texton-based approach for the classification of lung parenchyma in CT images. Medical Image Computing and Computer-Assisted Intervention – MICCAI 2010. Springer. 2010. 595–602
175. Dou Q, Chen H, Yu L, Qin J, Heng PA. Multilevel contextual 3-D CNNs for false positive reduction in pulmonary nodule detection. IEEE Trans Biomed Eng 2017; 64(7): 1558–1567
176. Torres EL, Fiorina E, Pennazio F, Peroni C, Saletta M, Camarlinghi N, Fantacci ME, Cerello P. Large scale validation of the M5L lung CAD on heterogeneous CT datasets. Med Phys 2015; 42(4): 1477–1489
177. van Ginneken B, Armato SG 3rd, de Hoop B, van Amelsvoort-van de Vorst S, Duindam T, Niemeijer M, Murphy K, Schilham A, Retico A, Fantacci ME, Camarlinghi N, Bagagli F, Gori I, Hara T, Fujita H, Gargano G, Bellotti R, Tangaro S, Bolaños L, de Carlo F, Cerello P, Cristian Cheran S, Lopez Torres E, Prokop M. Comparing and combining algorithms for computer-aided detection of pulmonary nodules in computed tomography scans: The ANODE09 study. Med Image Anal 2010; 14(6): 707–722
178. Rajpurkar P, Irvin J, Zhu K, *et al*. CheXNet: radiologist-level pneumonia detection on chest X-rays with deep learning. arXiv: Computer Vision and Pattern Recognition. arXiv preprint. 2017. arXiv:1711.05225
179. Yao L, Poblenz E, Dagunts D, *et al*. Learning to diagnose from scratch by exploiting dependencies among labels. arXiv: Computer Vision and Pattern Recognition. arXiv preprint. 2018 arXiv: 1710.10501
180. Jaeger S, Candemir S, Antani S, Wáng YXJ, Lu PX, Thoma G. Two public chest X-ray datasets for computer-aided screening of pulmonary diseases. Quant Imaging Med Surg 2014; 4(6): 475–477
181. Bi WL, Hosny A, Schabath MB, Giger ML, Birkbak NJ, Mehrtash A, Allison T, Arnaout O, Abbosh C, Dunn IF, Mak RH, Tamimi RM, Tempany CM, Swanton C, Hoffmann U, Schwartz LH, Gillies RJ, Huang RY, Aerts HJWL. Artificial intelligence in cancer imaging: clinical challenges and applications. CA Cancer J Clin 2019; 69(2): 127–157